

## Spatial Variability and Transport of Nitrate in a Deep Alluvial Vadose Zone

Yuksel S. Onsoy, Thomas Harter,\* Timothy R. Ginn, and William R. Horwath

### ABSTRACT

Little empirical evidence exists about the spatial distribution of  $\text{NO}_3\text{-N}$  in deep vadose zones and about the associated fate and transport of  $\text{NO}_3\text{-N}$  between the root zone and the water table. We investigated  $\text{NO}_3\text{-N}$  occurrence in a deep alluvial vadose zone and its relation to geologic site characteristics, hydraulic properties, and fertilizer application rates via an intensive three-dimensional core-sampling campaign beneath an irrigated orchard in semiarid Fresno County, California. Statistical and geostatistical analyses were used to determine spatial variability of  $\text{NO}_3\text{-N}$  and water content, to estimate total  $\text{NO}_3\text{-N}$  mass in the vadose zone beneath each of three fertilizer treatments, and to compare  $\text{NO}_3\text{-N}$  occurrence with that predicted from standard agronomic analysis of N and water flux mass balances. Vadose zone  $\text{NO}_3$  was highly variable and lognormally distributed. Fertilizer treatment had a significant effect on  $\text{NO}_3\text{-N}$  levels in the vadose zone. In all cases, deep vadose zone N mass estimated by kriging measured data totaled only one-sixth to one-third of the mass predicted by the N and water flux mass balance approach. Vadose zone denitrification estimates could not account for this discrepancy. Instead, the discrepancy was attributed to highly heterogeneous flux conditions that were not accounted for by the mass-balance approach. The results suggest that spatially variable vadose zone flow conditions must be accounted for to better estimate the potential for groundwater  $\text{NO}_3$  loading.

INTENSIVE USE OF agrochemicals such as fertilizers and pesticides has been recognized as a major source of nonpoint source pollution. Subsurface  $\text{NO}_3$  transport is of particular interest because of the widespread application of inorganic and manure based  $\text{NO}_3$  fertilizers. Highly mobile and persistent,  $\text{NO}_3$  has become a primary groundwater pollutant (USEPA, 1990; Lunn and Mackay, 1994; Bransby et al., 1998; Ling and El-Kadi, 1998). Between 1945 and 1993, the use of  $\text{NO}_3$  in commercial fertilizers in the USA increased 20-fold (Puckett, 1995). In semiarid regions with intensive irrigated agricultural production (e.g., in California and the southwestern USA), conflicts between water scarcity and  $\text{NO}_3$  groundwater pollution have further highlighted concerns about soil N management (Owens et al., 1992).

Driven in part by pollution prevention measures that attempt to optimize the use of fertilizers, N budgeting methods for specific crop-fertilizer application scenarios have been widely used in agronomy to determine the fate of N in soils and the potential for N leaching to groundwater (Tanji and Gupta, 1978; Frissel et al., 1981; Legg and Meisinger, 1982; Willigen and Neeteson, 1985). These methods are driven by experimental stud-

ies of N cycling processes that have almost exclusively focused on the uppermost soil horizon (0–30 cm, Paus-tian et al., 1990; Tindall et al., 1995; Watkins and Bar-clough, 1996; Simek and Kalcik, 1998; Sharmasakkar et al., 1999) or on the root zone (0–1.8 m, Lafolie et al., 1997; Trettin et al., 1999; de Vos et al., 2000; Allaire-Leung et al., 2001; Stenger et al., 2002). Some exper-iments examined the annual N budget with intensive field investigations, but were not of long enough dura-tion for a proper assessment of the effects of land man-agement practices on groundwater quality (e.g., Paus-tian et al., 1990; Aronsson, 2001).

Critical gaps remain in our understanding of the influ-ence of the vadose zone *below* the root zone, where it exists, on the estimation of N loading to aquifers (Ling and El-Kadi, 1998). Mechanisms involved in N transfer in the (deep) vadose zone below the root zone are rarely measured. The dearth of information about the deeper vadose zone results partly from the misconception that little chemical and biological activities occur below the root zone (i.e., below 0.3–1.8 m) (Pionke and Lowrance, 1991; Krug and Winstanley, 2002), but the vadose zone of many agricultural regions is considerably deeper and may contain appreciable amounts of organic matter (OM) or  $\text{NO}_3$  or both (Stevenson, 1986). Nitrate well below 1.8 m may be available to some plants (Smith and Cassel, 1991). Furthermore, denitrification between the root zone and the water table may significantly reduce N loading to groundwater, although this is difficult to quantify (Rees et al., 1995). Our current understanding of  $\text{NO}_3$  fate and transport below the root zone is further limited by pro-hibitive experimentation costs (e.g., Rees et al., 1995), by potentially long travel times through deep vadose zones, and perhaps most importantly, by a large degree of spatial variability.

Spatial variability is caused by spatially variable water and N application rates (i.e., external variability) and by spatially variable vadose zone hydraulic and chemical properties (i.e., intrinsic variability). Both may lead to highly nonuniform distribution of  $\text{NO}_3$  and other agro-chemicals (Rao and Wagenet, 1985; Mohanty and Kan-war, 1994). Past studies have quantified spatial varia-bility of  $\text{NO}_3$  by geostatistical methods, but only within the root zone of agricultural field soils (Dahiya et al., 1984; Tabor et al., 1985; White et al., 1987; van Meir-venne and Hofman, 1989; Istok et al., 1993; Cambardella et al., 1994; Hofman et al., 1994; Mohanty and Kanwar, 1994; Sharmasakkar et al., 1999; Allaire-Leung et al., 2001; Ilsemann et al., 2001; Stenger et al., 2002).

Equivalent field work on the spatial variability and storage of  $\text{NO}_3$  in the deep vadose zone (below the root zone) and analysis of its relationship to field-scale N mass balance and  $\text{NO}_3$  leaching into groundwater has,

Y.S. Onsoy1, T. Harter, T.R. Ginn, and W.R. Horwath, Department of Land, Air, and Water Resources, One Shields Avenue, University of California, Davis, CA 95616-8628. Received 26 Apr. 2004. Original Research Paper. \*Corresponding author (ThHarter@ucdavis.edu).

Published in Vadose Zone Journal 4:41–54 (2005).

© Soil Science Society of America

677 S. Segoe Rd., Madison, WI 53711 USA

**Abbreviations:** BNF, biological N fixation; K–S, Kolmogorov–Smirnov; MB, mass balance; OM, organic matter.

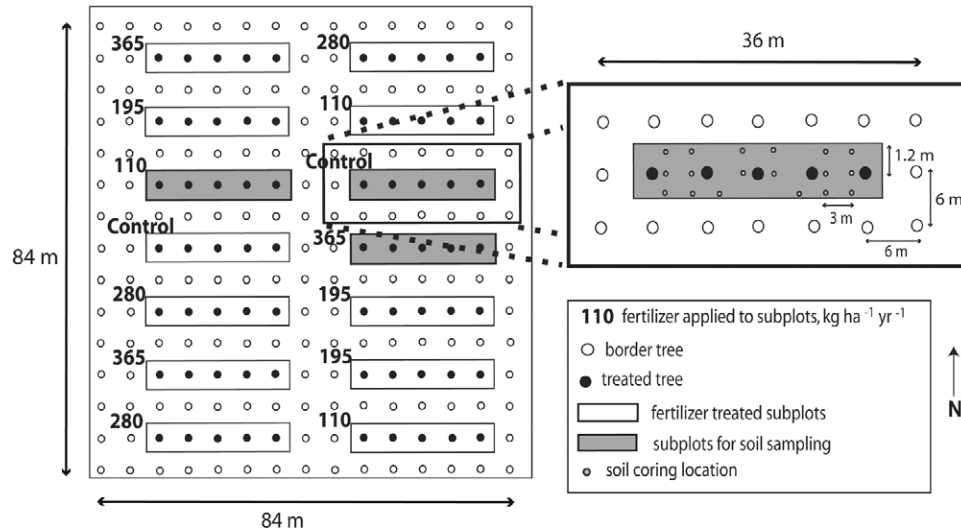


Fig. 1. The field experiment design showing the locations of five different fertilizer treatments at the project site. Three subplots with the 0, 110, and 365 kg N ha<sup>-1</sup> yr<sup>-1</sup> treatments were selected for vadose zone sampling. The three subplots were named “control,” “standard,” and “high,” respectively.

to our knowledge, not yet been attempted. The goal of our work is therefore to provide a detailed field analysis of NO<sub>3</sub> occurrence in a deep alluvial vadose zone, its relationship to the geologic and hydraulic characteristics of the vadose zone and to fertilizer management, and to discuss the implications of our findings with respect to common interpretations of vadose zone data.

Recognizing that the study is site specific, we do not make a strong claim that our results can be quantitatively transferred to other sites and situations. However, the general site conditions (alluvial soils, semiarid Mediterranean climate, irrigated crops) are representative of many important agricultural regions around the globe. The fundamental conditions at the study site, namely the strong heterogeneity of the NO<sub>3</sub> distribution, the lack of significant denitrification, and the strong control of the heterogeneous hydraulic and flow conditions on the NO<sub>3</sub> distribution are therefore not unique to this site and provide universal insight into “real” deep vadose zones. Therefore, findings from this site provide important evidence for the fate and transport of NO<sub>3</sub> in deep vadose zones in general. In particular, we hope that studies like the one presented here will provide a useful basis for developing guidance on the role of monitoring devices in the deep vadose zone.

In the following, we give a brief description of the site and the experimental methods. We then implement a conventional field-scale root zone water and N mass balance (MB) analysis to estimate NO<sub>3</sub>-N leaching from the root zone and to provide a predictive framework for the assessment of deep vadose zone NO<sub>3</sub>-N. A statistical analysis of the measured water content and NO<sub>3</sub>-N distribution is used to separate deterministic large-scale spatial variability that can be explained by depth, N treatment, and discrete lithofacies zonation from random smaller-scale spatial variability. For the nondeterministic residuals, we develop appropriate geostatistical models of the deep vadose zone water content and NO<sub>3</sub>-N data to estimate the total deep vadose zone

NO<sub>3</sub>-N mass. In the discussion, we compare this estimate with the total NO<sub>3</sub>-N mass predicted from the MB analysis to evaluate the deep vadose zone NO<sub>3</sub> fate and transport processes and the role of spatial variability in assessing potential NO<sub>3</sub> leaching to groundwater.

## METHODS

### Field Site

The site is a flood-irrigated, 0.8 ha (2 acres) ‘Fantasia’ nectarine [*Prunus persica* (L.) Batsch var. *nucipersica* (Suckow) C.K. Schneid. ‘Fantasia’] orchard at the University of California Kearney Agricultural Center (<http://www.uckac.edu>), located 20 km southeast of Fresno, CA, on the Kings River alluvial plain (elevation: 103 m above sea level). The site has a semiarid, Mediterranean climate.

### Fertilizer Treatments

Planted in 1975, the matured orchard was subject to a 12-yr fertilizer trial that began in September 1982. A complete random block design was used (Fig. 1) with application rates of 0, 110, 195, 280, or 365 kg N ha<sup>-1</sup> yr<sup>-1</sup> in several replicates. Fertilizer was broadcast in September of each year at a rate of 110 kg N ha<sup>-1</sup> to all rows except the control treatments (0 kg N ha<sup>-1</sup> yr<sup>-1</sup>). During the following spring, the 195, 280, and 365 kg N ha<sup>-1</sup> yr<sup>-1</sup> treatments received additional applications at a rate of 85 kg N ha<sup>-1</sup> (or 75 lb ac<sup>-1</sup>) once, twice, and three times, respectively, to achieve the desired annual fertilization rate. In the first year, (NH<sub>4</sub>)<sub>2</sub>SO<sub>4</sub> was applied. To prevent soil acidification, NH<sub>4</sub>NO<sub>3</sub> (33.5% N content) and Ca(NO<sub>3</sub>)<sub>2</sub> (15.5% N content) were used throughout the remainder of the study. There was no application of fertilizer in 1995. In September 1996, 110 kg N ha<sup>-1</sup> was applied throughout the entire orchard including the control plots in the usual broadcast application method. Vadose zone water quality analysis was not part of the original project’s scope.

### Irrigation and Climate Measurements

Flood irrigation dates were obtained from farm records at the Kearney Agricultural Center. Irrigation records indicate

that the approximate amount of applied water was  $13.4 \text{ cm ha}^{-1}$  ( $5.3 \text{ in ac}^{-1}$ ) per irrigation. Depending on spring precipitation patterns, 9 to 16 irrigations (average of 13 irrigations) were applied to the orchard each year. Daily reference evapotranspiration and precipitation data were measured at a California Irrigation Management Information System climate field station located within 1 km from the site. Crop evapotranspiration was computed from the product of the daily reference evapotranspiration rates and crop coefficients,  $k_c$ , for nectarine orchards (California Department of Water Resources, 2000). Over the past 20 yr, annual precipitation ranged from 160 to 490 mm, while groundwater levels during that period fluctuated between 12 and 20 m below ground surface.

### Yield and Plant Nitrogen Uptake

The nectarine orchard blossoms in mid- to late February immediately before leafing out. Fruit ripening is completed by July. Using standard methods, crop yield (fruit weight) and leaf N concentrations were measured in 1983 through 1985 and in 1991 through 1994. Fruit N concentrations were only measured in 1983 (Johnson et al., 1995).

### Vadose Zone Sampling

In 1997, three subplots with the 0, 110, and  $365 \text{ kg N ha}^{-1} \text{ yr}^{-1}$  treatments were selected for sampling (Fig. 1). For convenience, the three subplots are named "control," "standard," and "high," respectively, throughout the text. Between July and October 1997, 60 undisturbed continuous soil cores were drilled with a Geoprobe Systems (Salina, KS) direct-push drilling rig to a depth of 15.8 m (52 ft), including 18 cores from each subplot (Fig. 1). Cores were obtained in approximately 1.2-m sections (4 ft), their sedimentologic characteristics were described, and then the cores were sampled. More than 1000 soil samples of 22.5 cm long and 4 cm in diameter were taken at 30- to 60-cm intervals depending on stratification. Subsamples were prepared and preserved for later analysis. During the drilling phase, groundwater was detected at approximately 16 m below the ground surface.

### Vadose Zone Textures

The entire vadose zone at the site consists of unconsolidated sediments deposited on a stream-dominated alluvial fan. The textural groups range from clay and clayey paleosol hardpans to a wide range of silt and sand, including occasional coarse sand and gravel sediments. Coarse-grained materials are believed to represent channel deposits embedded within finer-grained floodplain and levee deposits. Sandy loam is the most common textural unit in the profile while clay was the least (48 and 8% of the vertical profile length, respectively). Ten major stratigraphic units were identified based on texture, color, and cementation and are referred to as "lithofacies." They exhibit vertically varying thicknesses, yet are laterally continuous across the experimental site. The measured saturated hydraulic conductivity data, best described by a lognormal distribution, indicate high hydraulic variability at the local scale ( $10^{-2}$ – $10^{-1} \text{ cm}$ , for details see Minasny et al., 2004).

### Soil Water Content and Nitrate

Gravimetric water content  $\theta_{\text{dw}}$  ( $\text{g g}^{-1}$ ) was determined using measured values of oven-dried ( $105^\circ\text{C}$  for 24 h) 1.25-cm (1/2-in)-long samples. Bulk density was measured on 119 core samples and varied from 1.3 to  $1.9 \text{ g cm}^{-3}$ , with an average of  $1.6 \text{ g cm}^{-3}$ . However, core samples, particularly finer-textured samples, were subject to variable compression during coring.

Therefore, a more representative constant bulk density  $\rho_b$  of  $1.45 \text{ g cm}^{-3}$  (Hausenbuiller, 1985) and the measured values of  $\theta_{\text{dw}}$  were used to compute volumetric water content  $\theta$  ( $\text{m}^3 \text{ m}^{-3}$ ). Regardless of the specific number used for bulk density, the potential error introduced is small ( $<10\%$ ) compared with the large range of observed  $\text{NO}_3$  concentrations (see below).

Nitrate concentration was measured in  $0.5 \text{ M K}_2\text{SO}_4$  soil extractions (5/1 ratio, 1-h reciprocal shaking) prepared from 809 core subsamples sieved through a 1-mm screen (Horwath and Paul 1994). Soil extracts were analyzed by automated flow-injection colorimetry following the methods of the USEPA 353.2 (Wendt, 1999). At each subplot, the smallest horizontal sampling interval varied between 1.2 to 3 m (10 and 4 ft, respectively, Fig. 1). The average vertical sampling interval was approximately 0.6 m (2 ft). Two hundred twenty-four sample concentrations were below the limit of detection ( $\text{LOD} = 10^{-3} \text{ mg L}^{-1} = 10^{-3} \text{ g m}^{-3}$ ) and recorded as zero. Measured values were converted to aqueous concentrations  $\text{NO}_3\text{-N}_{\text{aq}}$  in units of grams per cubic meter (or equivalently  $\mu\text{g mL}^{-1}$ ), using measured water content data. Both,  $\theta$  and  $\text{NO}_3\text{-N}_{\text{aq}}$  measurements contribute to the N mass estimate and are therefore both included in the statistical analysis. Results of core analyses for  $\theta$  and  $\text{NO}_3\text{-N}_{\text{aq}}$  are summarized in Table 1.

## FIELD-SCALE WATER AND NITROGEN FLUXES: NITROGEN BUDGET

The principle method for analyzing and predicting the  $\text{NO}_3$  leaching potential is a field- or plot-scale MB analysis coupled with a simple uniform steady-state flow model. We applied the method to provide a basis of comparison for the amount of  $\text{NO}_3\text{-N}$  in the deep vadose zone from the three subplots. The vadose zone was conceptually divided into two compartments: soil root zone and deep vadose zone (Fig. 2). The root zone is considered to be 1.8 m (6 ft) deep. Approximately 90% of the tree roots in the nectarine orchard are contained in this zone, with some roots to depths of 3 m (6–10 ft). Individual roots are expected to grow as long as 6 to 9 m (20–30 ft) horizontally (Scott Johnson, personal communication, 2004). The deep vadose zone is bounded by the soil root zone at the top and the water table at the 15.8-m depth. A long-term root zone N mass balance yields annual  $\text{NO}_3\text{-N}$  leaching,  $N_{\text{leaching}}$ , from the root zone into the deep vadose zone:

$$N_{\text{leaching}} = N_{\text{input}} - N_{\text{uptake}} - N_{\text{transformation}} - \Delta N \quad [1]$$

where  $N_{\text{input}}$  is the total N input to the root zone,  $N_{\text{uptake}}$  is the N used for plant uptake,  $N_{\text{transformation}}$  is the N loss through various N transformations in the root zone other than N leaching, and  $\Delta N$  is the change in the total amount of N (organic and inorganic) stored in the root zone.  $N_{\text{leaching}}$  is equivalent to the long-term potentially leachable N (LPLN) described in Meisinger and Randall (1991).

### Nitrogen Storage Changes

When soil, climate, and management factors are constant for an extended time (5–20 yr), annual mineralization of N from soil OM has been found to be approximately equivalent to organic N returned to the soil in crop residues plus microbial immobilization (Legg and Meisinger, 1982; Stevenson, 1982). Hence, annual changes in N storage reach a quasi-steady state,  $\Delta N \approx 0$  (Meisinger and Randall, 1991). Warm, semiarid climate conditions with irrigation further accelerate the time required for a system to reach quasi-steady-state conditions with respect to annual N storage changes. The 12-yr duration of the fertilizer treatment was considered sufficient to assume that annual N storage changes were negligible ( $\Delta N = 0$ ).

**Table 1.** Basic statistics of water content  $\theta$ , nitrate–nitrogen  $\text{NO}_3\text{-N}_{\text{aq}}$ , and logtransformed  $\text{NO}_3\text{-N}_{\text{aq}}$ . The number of samples measured for water content are: 339 in the control, 391 in the standard, and 310 in the high subplot. During the data quality check, 27 water content samples were removed due to inconsistencies (10 from both the control and standard subplots and 7 from the high subplot), which reduced the number of samples used in geostatistical analysis to 1013. Also shown are basic statistics of  $\text{NO}_3\text{-N}_{\text{aq}}$  and logtransformed  $\text{NO}_3\text{-N}_{\text{aq}}$  categorized by subplots.

Data	Subplot	No. of data	Mean	Min.	Max.	Variance	SD	CV	Mean	Variance	Skewness
$\theta$ , $\text{cm}^3 \text{cm}^{-3}$	–	1183	0.23	0.004	0.59	0.015	0.12	–	–	–	0.50
$\text{NO}_3\text{-N}_{\text{aq}}$ w/ND, $\text{g m}^{-3}\ddagger$	–	809	3.28	0	129.72	62.74	7.92	–	–	–	9.51
$\text{NO}_3\text{-N}_{\text{aq}}$ w/o ND, $\text{g m}^{-3}\ddagger$	–	585	4.54	0.04	129.72	81.10	9.00	–	–	–	8.55
$\ln\text{NO}_3\text{-N}_{\text{aq}}$ w/ND, $\text{g m}^{-3}\ddagger$	–	809	–0.70	–4.61	4.87	6.97	2.63	–	–	–	–0.53
$\ln\text{NO}_3\text{-N}_{\text{aq}}$ w/o ND, $\text{g m}^{-3}\ddagger$	–	585	0.80	–3.24	4.87	1.54	1.24	–	–	–	–0.46
$\text{NO}_3\text{-N}_{\text{aq}}$ w/ND, $\text{g m}^{-3}\ddagger$	control	204	3.73	–	–	80.64	8.98	241%	–	–	–
	standard	406	2.10	–	–	20.79	4.56	217%	–	–	–
	high	199	5.22	–	–	123.99	11.13	213%	–	–	–
$\text{NO}_3\text{-N}_{\text{aq}}$ w/o ND, $\text{g m}^{-3}\ddagger$	control	158	4.82	–	–	99.00	9.95	207%	–	–	–
	standard	277	3.08	–	–	27.48	5.24	170%	–	–	–
	high	150	6.93	–	–	152.86	12.36	178%	–	–	–
$\ln\text{NO}_3\text{-N}_{\text{aq}}$ w/ND, $\text{g m}^{-3}\ddagger$	control	204	–0.51	–	–	6.40	2.53	NA§	NA§	NA§	–
	standard	406	–1.06	–	–	6.69	2.59	NA§	NA§	NA§	–
	high	199	–0.15	–	–	7.57	2.75	NA§	NA§	NA§	–
$\ln\text{NO}_3\text{-N}_{\text{aq}}$ w/o ND, $\text{g m}^{-3}\ddagger$	control	158	0.69	–	–	1.91	1.38	240%§	5.17§	153.66§	–
	standard	277	0.59	–	–	1.22	1.11	155%§	3.31§	26.11§	–
	high	150	1.30	–	–	1.41	1.19	176%§	7.43§	170.66§	–

† Including nondetects, ND, which are set to zero for  $\text{NO}_3\text{-N}_{\text{aq}}$  data and to half the limit of detection (–4.605) for  $\ln\text{NO}_3\text{-N}_{\text{aq}}$ .

‡ Excluding nondetects.

§ Sample  $\text{NO}_3\text{-N}_{\text{aq}}$  mean,  $m$ , and variance,  $s^2$ , estimated from mean,  $\mu$ , and variance,  $\sigma^2$ , of the logtransformed dataset:  $m = \exp(\mu + 0.5 \sigma^2)$  and  $s^2 = m^2[\exp(\sigma^2) - 1]$ . Coefficient of variation estimated for  $\text{NO}_3\text{-N}_{\text{aq}}$  sample mean and variance. NA: No estimates were computed from  $\ln\text{NO}_3\text{-N}_{\text{aq}}$  data with the nondetects included at –4.605 because the bimodal distribution of that dataset violates the normality assumption.

### Nitrogen Inputs

Annual N inputs included fertilizer applications, and N received from irrigation, precipitation, dry deposition, and nonsymbiotic  $\text{N}_2$  fixation. Table 2 lists average annual N inputs and margin of errors (95% confidence intervals) in the N mass balance analysis (e.g., Berthouex and Brown, 1994). Average  $\text{NO}_3\text{-N}$  concentration in irrigation water was  $4 \text{ g m}^{-3}$  (Harter et al., 1999). Long-term average annual irrigation N input is therefore  $70 \text{ kg N ha}^{-1} \text{ yr}^{-1}$ . A margin of error of  $\pm 10\%$  primarily accounts for the lack of precise irrigation flow measurements and also for measurement errors of the  $\text{NO}_3\text{-N}$  concentration.

Wet and dry depositions and biological N fixation at the site are considered secondary N inputs because of their small contribution to the N budget. Wet and dry depositions were estimated as 2 and  $14 \text{ kg N ha}^{-1} \text{ yr}^{-1}$ , respectively, based on data collected by the California Acid Deposition Monitoring Program at the nearest monitoring stations to our site, Lindcove, Tulare County and Bakersfield, Kern (e.g., Blanchard

and Tonnessen, 1993; Mutters, 1995). Biological N fixation (BNF) is small due to readily available N, low OM, and the lack of plant growth that supports N-fixing bacteria fertilization. Stevenson (1982) reported BNF inputs to be in the range of 2 to  $7 \text{ kg N ha}^{-1} \text{ yr}^{-1}$ .

### Nitrogen Plant Uptake and Transformations

In the first year of the experiment, there were no significant differences in yield or average fruit weight among the subplots. In the second and third years, the control subplot dropped off in both yield and fruit size, but then remained at about the same level for the duration of the experiment. The 7-yr average yield was 36, 51, and  $48 \text{ t ha}^{-1}$  for the control, standard, and high subplots, respectively, indicating a negative response of the high subplot to overfertilization. Nitrogen content in dry fruit measured in 1983 was 0.71, 1.51, and 2.05% for the control, standard, and high subplots, respectively. Nitrogen uptake estimates are based on 7-yr average annual crop yield and the dry matter fruit N content measured in 1983:

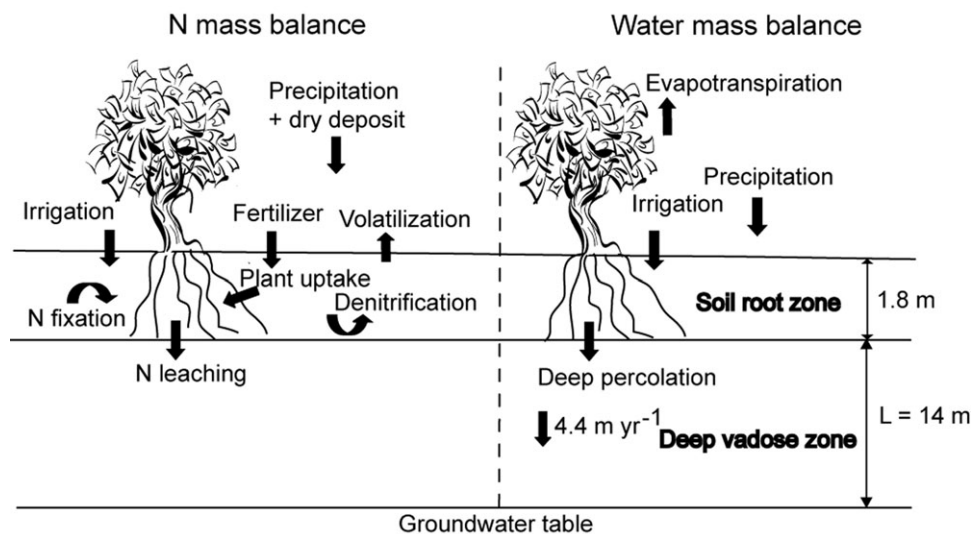


**Fig. 2.** A schematic representation of the components of the N budget and water mass balance.

**Table 2. Root zone water balance, root zone N mass balance, and deep vadose zone N storage estimation by the mass balance method. The 95% confidence intervals are given in parentheses. For computed results, confidence intervals were obtained by standard, linear error analysis (Berthouex and Brown, 1994). Confidence intervals for deep vadose zone storage were computed at the lower and upper 95% confidence intervals for the mean travel time through the deep vadose zone, given the confidence intervals of  $N_{\text{leaching}}$  and recharge.**

	Control	Standard	High	All 3 subplots
<b>Root zone water balance</b>				
Irrigation $I$ , cm yr <sup>-1</sup>				174 (157/192)
Precipitation $P$ , cm yr <sup>-1</sup>				33 (32/35)
Evapotranspiration $ET$ , cm yr <sup>-1</sup>				98 (93/103)
Recharge = $I + P - ET$ , cm yr <sup>-1</sup>				110 (91/128)
<b>Root zone N balance</b>				
<b>Primary inputs</b>				
Fertilizer appl., kg ha <sup>-1</sup> yr <sup>-1</sup> †	0	110	365	
Irrigation, kg ha <sup>-1</sup> yr <sup>-1</sup> †	70 (56/84)	70 (56/84)	70 (56/84)	
<b>Secondary inputs</b>				
Precipitation + dry deposit, kg ha <sup>-1</sup> yr <sup>-1</sup> ‡	16 (11/21)	16 (11/21)	16 (11/21)	
Nonsymbiotic N fixing, kg ha <sup>-1</sup> yr <sup>-1</sup> ‡	5 (2/7)	5 (2/7)	5 (2/7)	
Total, kg ha <sup>-1</sup> yr <sup>-1</sup>	91	201	456	
<b>Primary outputs (transformations)</b>				
Plant N uptake, kg ha <sup>-1</sup> yr <sup>-1</sup> †	25 (19/37)	77 (65/82)	98 (74/112)	
NH <sub>3</sub> losses, kg ha <sup>-1</sup> yr <sup>-1</sup> ‡	–	11 (2/22)	37 (7/73)	
Denitrification, kg ha <sup>-1</sup> yr <sup>-1</sup> ‡	9 (2/27)	20 (4/60)	46 (9/137)	
<b>Secondary outputs</b>				
Soil erosion + surface runoff, kg ha <sup>-1</sup> yr <sup>-1</sup>	–	–	–	
Total, kg ha <sup>-1</sup> yr <sup>-1</sup>	34	108	181	
<b>ΔN change in organic/inorganic N pool, kg ha<sup>-1</sup> yr<sup>-1</sup></b>				
$N_{\text{leaching}} = \text{inputs} - \text{outputs} + \Delta N$ , kg ha <sup>-1</sup> yr <sup>-1</sup>	57 (36/78)	93 (59/127)	275 (228/322)	
Potentially leachable N (LPLN) risk	low	medium	high	
<b>Deep vadose zone N storage</b>				
Measured, kg ha <sup>-1</sup>	48 (42/62)	36 (33/47)	87 (79/107)	
Predicted for 1997, kg ha <sup>-1</sup>	218 (130/334)	261 (147/427)	478 (271/784)	

† Measured.

‡ Estimated from literature reference values.

$$N_{\text{uptake}} = (\text{annual yield} \times 10\%) \times (\%N_{\text{content}}/100) \quad [2]$$

where 10% is the dry matter content in the fresh fruit. In the absence of multiyear measurements, fruit N concentrations (but not yield) were assumed to vary proportional to leaf N content (Scott Johnson, personal communication, 2004), which remained practically constant throughout the experiment. Annual yields varied among the 7 yr that N leaf content was measured. The measured range of annual yields provided a conservative basis for estimating the 95% confidence interval of the long-term average annual N uptake (Table 2).

Nitrogen in tree leaves is considered to be completely recycled into the root zone. Losses due to soil erosion and surface runoff are negligible since the ground surface at the orchard is flat and the basin irrigation system (surface flooding) generates no surface water return flow.

Denitrification and NH<sub>3</sub> losses were estimated from previous experimental studies (Meisinger and Randall, 1991) that took into account various controlling site conditions (e.g., irrigation, drainage, climate, soil OM, and pH). The observed range of 6 to 20% N loss from denitrification is consistent with the experimental findings of Dowdell and Webster (1984), who reported N loss of 2 to 19% during a long-term N balance study, but lower than the 15 to 30% loss estimates reported by Allison (1966) and Hauck (1981). We adopted an average N loss of 10% of  $N_{\text{inputs}}$  with the error margins equal to the range of reported loss percentages (2–30%, Table 2). Neutral to slightly acidic soil pH conditions at the site (not shown here) keep NH<sub>3</sub> volatilization at a minimum (Paustian et al., 1990). Average volatilization losses are approximately 10% with error margins equivalent to those of denitrification (Table 2) (Meisinger and Randall, 1991).

## Water Mass Balance and Deep Vadose Zone Nitrogen

The average annual water budget, as illustrated in Fig. 2, is (Martin et al., 1991)

$$R = I + P - ET \quad [3]$$

where  $R$  (m yr<sup>-1</sup>) is the average annual deep percolation (recharge) from the root zone, and  $I$ ,  $P$ , and  $ET$  (m yr<sup>-1</sup>) are average annual irrigation, precipitation, and (crop) evapotranspiration amounts for the 12 yr from 1984 to 1995. In the deep vadose zone, water flux is typically assumed to be at steady state and equal to the average water leaching rate from the root zone.

For predictive purposes, we applied a commonly used simple one-dimensional uniform steady-state flow concept. Average NO<sub>3</sub>-N concentration (g m<sup>-3</sup>) in the 14-m-deep vadose zone was obtained by multiplying annual NO<sub>3</sub>-N leaching loss from the root zone with the recharge rate  $R$ . The total amount of NO<sub>3</sub>-N (kg ha<sup>-1</sup>) contained within the deep vadose zone was computed by multiplying the annual NO<sub>3</sub>-N leaching loss,  $N_{\text{leaching}}$ , with the average time of travel,  $\tau$ , through the deep vadose zone, where  $\tau = 14 \text{ m} \times \theta_{\text{avg}}/R$ , and  $\theta_{\text{avg}}$  is the average reported field capacity (25%) for the dominant soil texture (Martin et al., 1991).

## STATISTICAL AND GEOSTATISTICAL ANALYSIS

### Statistical Analysis

Statistical analysis was used to determine sample distributions and to identify deterministic factors controlling the spa-

tial variability of water content  $\theta$  and  $\text{NO}_3\text{-N}_{\text{aq}}$ . Factors considered included depth,  $N$  treatments, and lithofacies distribution.

Depth-dependent trends were determined using a separate regression analysis of the  $\theta$  and logtransformed  $\text{NO}_3\text{-N}_{\text{aq}}$  for each subplot treatment. After removing trends, a Kolmogorov–Smirnov (K–S) test (e.g., Davis, 1986; Olea, 1999) was used to test normality of the  $\theta$  and logtransformed  $\text{NO}_3\text{-N}_{\text{aq}}$  distribution. The effects of subplot treatment (three groups: control, standard, and high) and lithofacies (10 sample groups, one for each lithofacies), and their interactions (30 groups) on  $\theta$  and  $\ln\text{NO}_3\text{-N}_{\text{aq}}$ , were measured by a sigma-restricted ANOVA with effective hypothesis decomposition (Hocking, 1985) to account for the unbalanced design (unequal number of samples between groups). Homogeneity of variance was assumed if the ratio of the largest to smallest group standard deviation did not exceed 3. Where significant effects were observed ( $p < 0.05$ ), Newman-Keuls and Duncan's multiple range tests were performed for post-hoc pair-wise comparison of means. Nitrate- $N$  samples below the LOD were not included in the significance analysis. To check for potential bias from exclusion of nondetects, a nonparametric Kruskal–Wallis ANOVA was performed on the bimodally distributed dataset with nondetect samples recorded at one-half the LOD concentration (see below). A Kruskal–Wallis test was also performed to test for significant effects of subplot and vertical location on the probability of nondetects (using an indicator variable of 1 for “non-detects” and 0 for “detects”). All statistical analyses were performed with the Statistica software (Statsoft, 2002).

### Geostatistical Analysis of Water Content and Nitrate Data

After trends were removed and appropriate variable transformations were done based on the results of the statistical analysis, geostatistical analysis was used (i) to quantify the amount of spatial variability in the  $\theta$  and  $\text{NO}_3\text{-N}$  distributions unexplained by depth, treatment, and lithofacies location; (ii) to characterize differences in the  $\text{NO}_3\text{-N}$  distribution among the three different fertilizer treatments; and (iii) to quantify the field-scale  $N$  loading rate to groundwater from those local-scale measurements. The correlation coefficient between  $\text{NO}_3\text{-N}_{\text{aq}}$  and  $\theta$  was  $-0.11$ ; hence,  $\theta$  and  $\text{NO}_3\text{-N}_{\text{aq}}$  were considered uncorrelated for purposes of the geostatistical analysis. Due to a large number of nondetect  $\text{NO}_3$  concentrations, two sets of experimental  $\text{NO}_3\text{-N}_{\text{aq}}$  semivariograms were computed for the complete dataset and for the dataset that excluded nondetects.

Directional (horizontal and vertical), nested spherical semivariograms were fitted to the observed semivariograms by initially using a manual calibration followed by a least square optimization process (e.g., Davis, 1986; Olea, 1999). Directional semivariograms were constructed with appropriate lag intervals that were assigned according to average horizontal and vertical sampling scheme (Fig. 1).

Ordinary block kriging (Deutsch and Journel, 1992) was applied to estimate average volumetric block values of  $\ln\text{NO}_3\text{-N}_{\text{aq}}$  and residual (i.e., trend-removed)  $\theta$  from their point measurements. The kriging domain size for each subplot was  $x = 24$  m,  $y = 3$  m, and  $z = 16$  m (80, 10, and 53 ft, respectively), discretized into blocks with  $\Delta x = 0.75$  m,  $\Delta y = 0.3$  m, and  $\Delta z = 0.15$  m.

## RESULTS

### Field-Scale Water and Nitrogen Balance: Long-Term Potentially Leachable Nitrogen

As expected, LPLN increases with  $N$  application rates since crop  $N$  uptake consumes only part of the increased

amount of  $N$  fertilizer (Table 2). The LPLN computed for the high subplot represents a potentially high risk for groundwater pollution (Meisinger and Randall, 1991). The net percolating water to below the root zone ( $R$ ) is  $1.1 (\pm 0.2)$  m  $\text{yr}^{-1}$  (Table 2), reflecting the low irrigation efficiency of the flood irrigation. The margin of error stems mostly from the large uncertainty about the mean irrigation rate, which was much larger than that for precipitation or crop evapotranspiration. The estimated net annual mean vertical solute travel distance is  $4.4 (\pm 0.8)$  m ( $\theta_{\text{avg}} = 25\%$ ) and the mean travel time to groundwater,  $\tau$ , is  $3.2 (2.8\text{--}3.8)$  yr (Fig. 2). At  $\tau = 3.2$  yr, field-scale  $N$  concentration in the leachate (and recharge) is predicted to be 5, 9, and  $25$  g  $\text{m}^{-3}$  for the control, standard, and high subplots, respectively. Corresponding deep vadose zone  $N$  storage is predicted to be 180, 300, and  $880$  kg  $\text{N ha}^{-1}$ , respectively. For 1997, the deep vadose zone storage can be computed by considering that all subplots were subject to the “control” leaching rate in 1995 (no fertilizer application) and to the “standard” leaching rate in 1996 (uniform standard fertilizer application). Then, the predicted deep vadose zone  $N$  storage at the time of drilling in 1997 is 220, 260, and  $480$  kg  $\text{N ha}^{-1}$ . The wide confidence intervals for the deep vadose zone  $N$  storage, summarized in Table 2, reflect potential errors in both the recharge and the LPLN computation.

### Statistical Analysis of Water Content and Nitrate Distribution

#### Water Content

Measured water content data follow an approximately symmetric, normal distribution (Table 1). Within all subplots water content is characterized by a significant linear increase with depth. Separate linear trend models were fit to each subplot dataset, as illustrated in Fig. 3. Trend residuals are shown to be normally distributed with K–S differences insignificant at the  $p = 0.1$  significance level. Trends are essentially identical between the three subplots.

Water content residuals are significantly controlled by lithofacies (ANOVA testing,  $p < 0.05$ ). Multiple range tests suggest that the thick sand S unit at approximately the 6- to 9-m depth is significantly drier (Fig. 3). Similarly, although only few samples were available, the clay and silt-textured C unit (from 2.75–3 m) and a clay-textured unit in Var3 (from 9–9.75 m) were found to be significantly wetter than the other lithofacies. Differences reflect varying field capacity between coarse, intermediate, and fine-textured lithofacies.

#### Nitrate

The  $\text{NO}_3\text{-N}_{\text{aq}}$  distribution is highly skewed (Fig. 4a) and lognormal (significance level,  $p < 0.05$ ) after excluding nondetect samples (Fig. 4b). Resulting sample means (estimated from the moments of the logtransformed data, Table 1) are 5.2, 3.3, and  $7.4$  g  $\text{m}^{-3}$  for the control, standard, and high subplots, respectively. Detectable  $\text{NO}_3\text{-N}_{\text{aq}}$  concentrations range from 0.04 to  $129.72$  g  $\text{m}^{-3}$

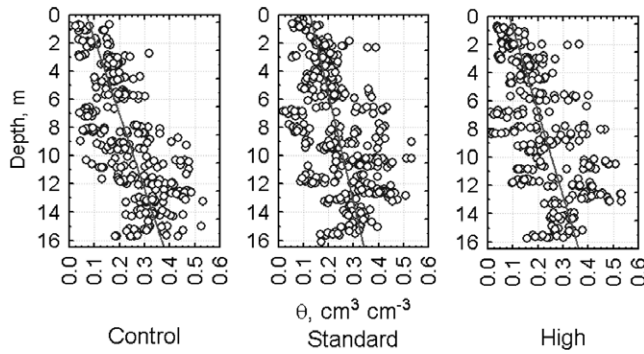


**Fig. 3.** Scatter plots of water content with depth for each subplot. Line represents linear regression models for the trend defined as a function of depth. Equations for the trends are  $\theta_c = 0.069 + 0.019z$  for the control subplot (a correlation coefficient of  $r^2 = 0.48$ ),  $\theta_s = 0.127 + 0.013z$  for the standard subplot ( $r^2 = 0.25$ ), and  $\theta_h = 0.087 + 0.017z$  for the high subplot ( $r^2 = 0.36$ ).

(Table 1). Of the samples with detectable concentrations, 21% measure  $<1 \text{ g m}^{-3}$  and 10% exceed the maximum contamination level for drinking water ( $10 \text{ g m}^{-3}$ ). Significant differences exist between subplots. In the high subplot, the fraction of low  $\text{NO}_3\text{-N}_{\text{aq}}$  measurements is less than one-third of the fraction observed in the other two subplots. On the other hand, most of the high concentration samples, exceeding  $10 \text{ g m}^{-3}$ , are found in the high subplot, while only a small fraction (8%) of these are found below the root zone of the control plot.

Figure 5a shows the profiles of lithofacies-specific mean  $\ln\text{NO}_3\text{-N}_{\text{aq}}$  in the three subplots. The lithofacies effect represents the combined influence of depth and sediment texture on  $\text{NO}_3\text{-N}_{\text{aq}}$  since the lithofacies are sorted in vertical sequence. At all three subplots, the highest average  $\text{NO}_3\text{-N}_{\text{aq}}$  levels occur in the root zone to approximately 3 m, which is mostly comprised of a fine sandy loam lithofacies (SL1). Below SL1,  $\text{NO}_3\text{-N}_{\text{aq}}$  concentrations are lower, but no significant vertical trends or contrasts were observed. The high subplot shows the largest  $\text{NO}_3\text{-N}_{\text{aq}}$  mean concentrations throughout most of the profile, which is consistent with the higher fertilizer applications. Differences between the control and standard subplot means are not significant. Coefficients of variation for each subplot range from 1.6 to 2.4 (Table 1) and similarly for individual lithofacies and lithofacies X subplot groups.

Almost one-third of the samples (28% of all samples) have nondetectable levels of  $\text{NO}_3\text{-N}_{\text{aq}}$  (Fig. 5b): 22% of the control, 32% of the standard, and 25% of the high subplot, and from 13% to 50% for individual facies. The fewest nondetects were observed at depths below 12 m (SL2, HP2) (Fig. 5b). The highest fractions of nondetects occurred in the coarse-textured, sandy lithofacies Var1, in the hardpan HP1, and in the sand lithofacies S, where approximately one-half of the samples had nondetectable levels of  $\text{NO}_3\text{-N}_{\text{aq}}$ .

Because of the large number of nondetects, replacing nondetects with a default value of  $-4.605$  (one-half of the LOD) leads to a bimodal  $\ln\text{NO}_3\text{-N}_{\text{aq}}$  distribution; the LOD for  $\text{NO}_3\text{-N}_{\text{aq}}$  is significantly lower than the extent of the left tail of the  $\ln\text{NO}_3\text{-N}_{\text{aq}}$  distribution in Fig. 4b. In other words, the number of nondetects (224)

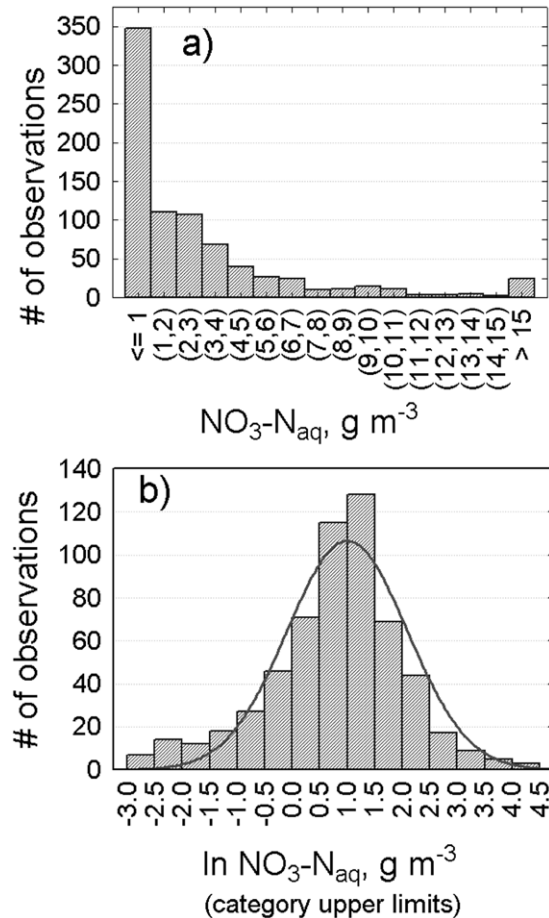


**Fig. 4.** (a) Frequency distribution of  $\text{NO}_3\text{-N}_{\text{aq}}$  ( $\text{g m}^{-3} = \mu\text{g mL}^{-1}$ ) (includes 224 nondetects in the left-most class). (b) Logtransformed  $\text{NO}_3\text{-N}_{\text{aq}}$  data fitted to a normal distribution with a mean of 1.0 and variance of 1.095 (does not include nondetects).

far exceeds the (small) number that would be expected if the fitted lognormal distribution of Fig. 4b is considered to be censored to the left. Because of the large number of nondetects, the first two sample moments of  $\ln\text{NO}_3\text{-N}_{\text{aq}}$  strongly depend on the concentration specified for nondetects (here one-half of LOD). Effectively then, the mean and variance become a measure of the mid-point and spread between the mode of the detect group and the level specified for the nondetect group (Table 1).

### Geostatistical Analysis of Water Content and Nitrate Distribution

Separate water content and  $\text{NO}_3$  semivariograms were computed for each subplot. Data density was not sufficient to derive well-structured separate semivariogram models for individual lithofacies within each subplot. But by applying a thin vertical bandwidth ( $<15 \text{ cm}$ ) in the search window, horizontal semivariograms were computed for data pairs containing only points within the same lithofacies (e.g., Deutsch and Journel, 1992).

#### Water Content

Semivariograms of the water content trend residuals exhibit not only a significant geometric anisotropy (un-

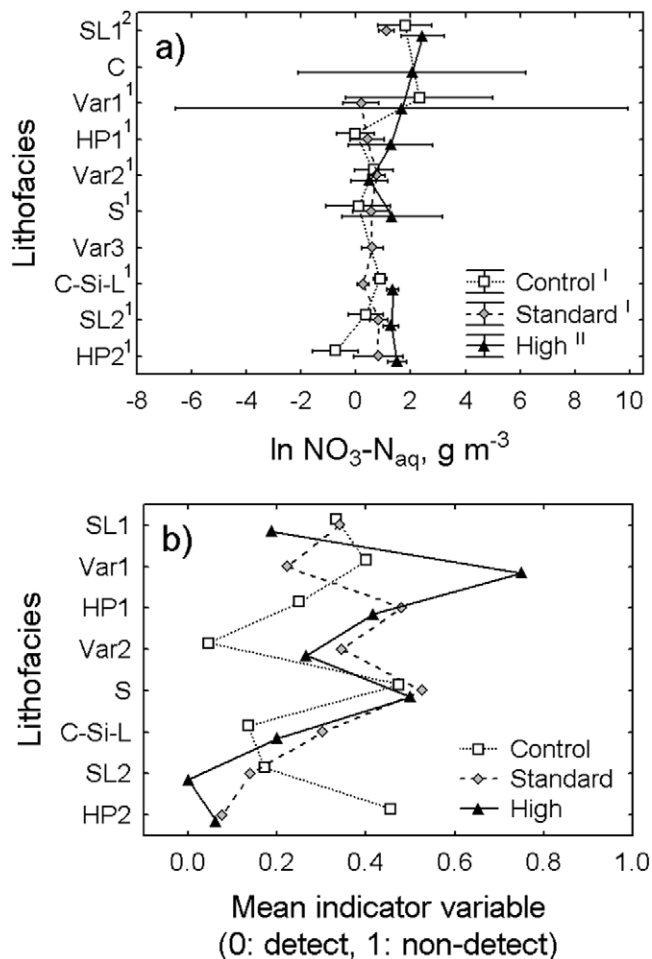


**Fig. 5.** (a) Facies X subplot group means and 95% confidence intervals for natural logtransformed  $\text{NO}_3\text{-N}_{\text{aq}}$  ( $\text{g m}^{-3}$ ), not including nondetect samples. Facies are sorted in vertical sequence followed by their average depth interval in meters given in parentheses: SL1, sandy loam (0–2.75); C, clay (2.75–3); Var1, thin, predominantly sand (2.75–3); HP1, hardpan-like paleosol (3–3.65); Var2, various sandy loam to clay loam (3.65–6.7); S, medium sand (6.7–9); Var3, various textures (9–9.75); C-Si-L, fine-textured floodplain deposits (9–12); SL2, sandy loam (12–15); and HP2, a hardpan-like paleosol (15–15.85). Lithofacies symbols followed by the same numbers (1, 2) indicate no significant differences between lithofacies groups at the 95% significance level (C and Var3 had less than four samples and those were from only one subplot and were therefore not included in the ANOVA). Fertilizer treatments (control, standard, high) followed by the same Roman numerals (I, II) indicate no significant difference between the fertilizer treatments at the 95% significance level. (b) Facies X subplot group means of the detect-nondetect indicator variable, that is, the fraction of nondetects in each group. No means were computed for C and Var3.

equal range), but also a strong zonal anisotropy (unequal sill) throughout all subplots. The sill in the horizontal direction (Fig. 6a–6c) is significantly smaller, while the range in the horizontal direction is significantly longer than in the vertical direction (Fig. 6d–6f).

Kriged  $\theta$ , shown in Fig. 7, is much less variable than the distribution of  $\text{NO}_3\text{-N}_{\text{aq}}$  (see below). Due to the large horizontal correlation scale, water content distribution is fairly uniform, with predominantly horizontal layering (e.g., Hills et al., 1991). Although all three subplots exhibit a similar trend of soil moisture distribution, the depth profiles of water content data shown in Fig. 7b

suggest that the deeper portion of the control and high subplots is wetter than that of the standard subplot.

### Nitrate

Separate semivariograms for the complete dataset and for the detectable level dataset were computed and, for comparison, plotted after normalizing the semivariograms by their respective variances (Fig. 8). The semivariogram of the complete dataset with its strong bimodal distribution and large standard deviation (2.63, see Table 1) reflects the combined effect of two spatial variability structures: (i) the spatial variability structure between measurable  $\ln \text{NO}_3\text{-N}_{\text{aq}}$  levels (pattern of different colors in Fig. 9) and (ii) the spatial variability of the bimodal pattern of zones with nondetectable  $\text{NO}_3\text{-N}_{\text{aq}}$  and zones with detectable  $\text{NO}_3\text{-N}_{\text{aq}}$  (pattern of purple/dark vs. other colors in Fig. 9). Separate variograms were computed for the two datasets, to determine whether the pattern created by the bimodality dominated the semivariogram structure because of the large concentration difference between the two modes in the distribution. However, the normalized semivariograms of the two datasets were found to be essentially identical. Only the vertical nugget effect, especially in the high subplot, is notably smaller for the semivariograms of the smaller (detectable levels only) dataset. Hence, vertical spatial continuity is higher within zones of measurable  $\text{NO}_3\text{-N}_{\text{aq}}$  (triangles) than between zones of measurable and nondetectable  $\text{NO}_3\text{-N}_{\text{aq}}$  (diamonds). In the horizontal direction, differences between the two sets of semivariograms are not significant.

Kriged concentrations (using the semivariograms of the complete dataset) are found to be highly variable with several “plumes” of high concentration observed near the top and in the upper third of the profile of each subplot (Fig. 9). The total N mass in the vadose zone obtained from kriging is  $52 (\pm 9.7)$ ,  $40 (\pm 7)$ , and  $93 (\pm 14.1)$  kg N ha<sup>-1</sup> for the control, standard, and high subplots, respectively. Confidence intervals represent the average kriging error variance. The deep vadose N mass (without the root zone) is 48, 36, and 87 kg N ha<sup>-1</sup>, respectively. These latter kriged (“measured”) total N masses amount to 24% (15–40%), 15% (9–27%), and 19% (12–34%), respectively, of those predicted from the MB analysis for 1997 (values in parentheses account for estimation errors in the MB analysis).

These observations raise several issues to be discussed in the following section: What are the potential errors contributing to the difference between predicted and measured deep vadose zone N? How representative and significant is the amount of observed spatial variability of water content and  $\text{NO}_3$ ? What does the observed spatial variability of water content and  $\text{NO}_3$  indicate with respect to the spatial distribution of water flux and the expected fate of transport?

## DISCUSSION

### Measured vs. Predicted Nitrate Mass in the Deep Vadose Zone

Several reasons may explain the large discrepancy between the two estimates of deep vadose zone  $\text{NO}_3$ :

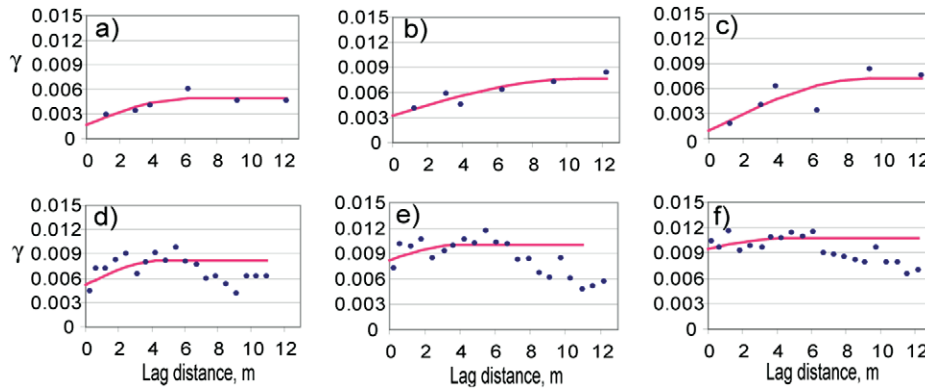


**Fig. 6.** Experimental and spherical model semivariograms for water content (trend residuals) in the horizontal direction for the (a) control, (b) standard, and (c) high subplot; and in the vertical direction for (d) the control, (e) standard, and (f) high subplot. Diamonds denote experimental values and lines denote spherical semivariogram models.

estimation errors in the MB method yielding an erroneous interpretation for LPLN, estimation errors in the geostatistical analysis of vadose zone N mass, significant N losses in the deep vadose zone not accounted for in

the MB method, and nonuniform flow conditions in the vadose zone.

The computed error margins for recharge, LPLN, and the resulting deep vadose zone storage (Table 2) are on the same order as the 30% of actual leaching losses suggested by Meisinger and Randall (1991). Although large, neither these errors nor those from the kriging analysis can explain the observed difference between MB predicted and measured deep vadose zone N.

If the differences were assumed to be primarily caused by denitrification (Bar-Yosef and Kafkafi, 1972; Aronson, 2001) under predominantly uniform vertical flow conditions, the amount of N loss in the deep vadose zone should be on the order of one hundred to several hundred kilograms per hectare within one leaching cycle (i.e., 3.2 yr) with much higher denitrification rates under the high subplot than the other two subplots. Most of this denitrification would have had to occur in the shallowest zone because no significant depth-dependent decrease in  $\text{NO}_3\text{-N}$  was observed below the root zone and because several relatively high  $\text{NO}_3\text{-N}$  concentrations were measured even at depth. However, denitrification rates of more than 55 to 60  $\text{kg ha}^{-1} \text{yr}^{-1}$  are unlikely, given the low organic C content of the root zone and its relatively coarse texture (e.g., Rolston et al., 1982; Aronsson, 2001; Sanchez et al., 2001; Krug and Winstanley, 2002). This is also consistent with the lack of significant vertical trends in the N isotope fractionation observed at the site (Harter et al., 2004).

While the denitrification processes in the deep vadose zone may be locally significant (Harter et al., 2004), other explanations, namely the role of heterogeneity and flow nonuniformity (not considered in the MB model) must be considered to explain the large discrepancy between field measured and MB estimated deep vadose zone N content. The site stratigraphy and hydraulic properties are highly variable both between facies and within facies (Minasny et al., 2004). The significant degree of layering observed at the site is typical of the alluvial fan architecture in the region, which contains laterally extensive hardpans and floodplain deposits intercalated between higher permeable sediments of varying texture representing channel and overbank deposits (Page and LeBlanc, 1969; Weismann et al., 1999). While

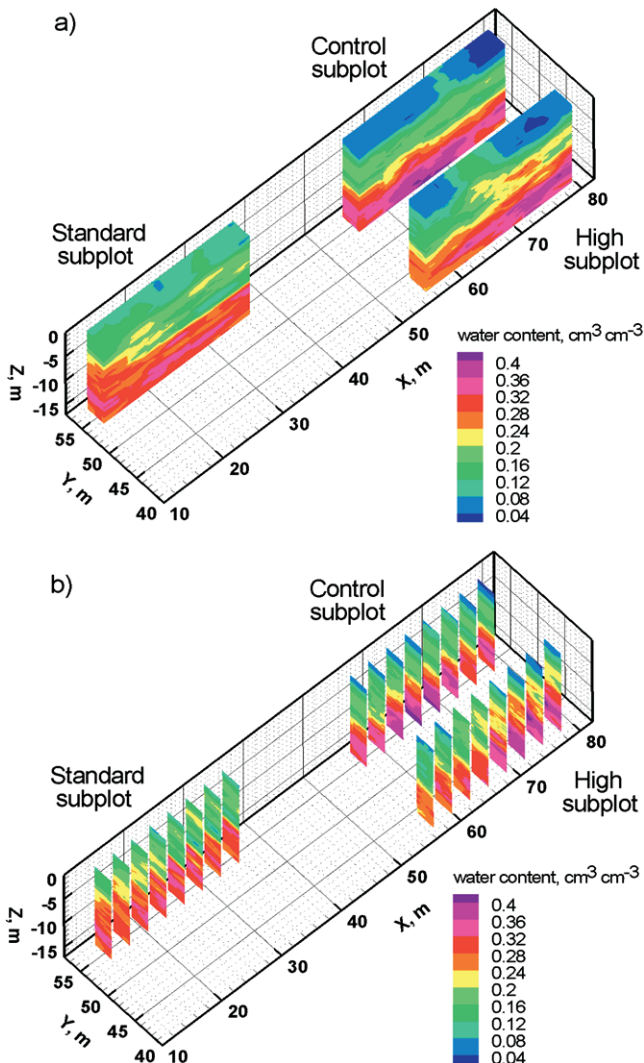


**Fig. 7.** Contour maps of the kriged (a) water content at the control, standard, and high fertilizer treatment sites; (b) various depth profiles of water content at each subplot.

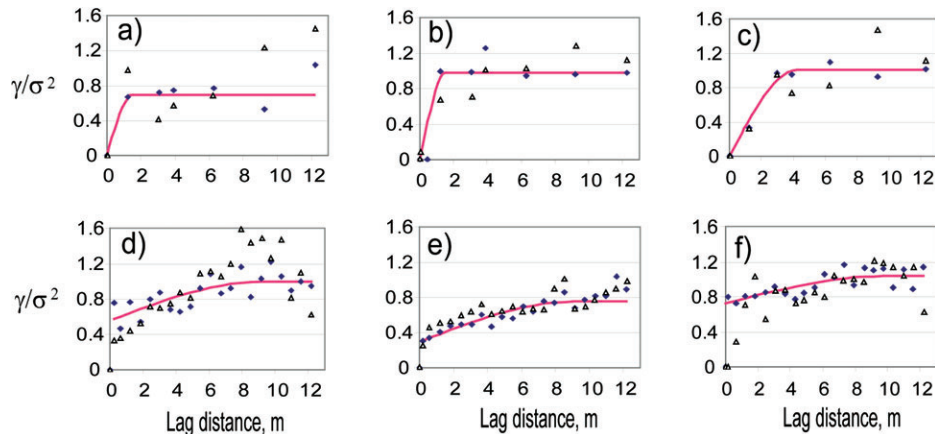


Fig. 8. Normalized experimental and spherical model semivariograms for  $\ln\text{NO}_3\text{-N}_{\text{aq}}$  in the horizontal direction for the (a) control, (b) standard, and (c) high subplot and in the vertical direction for the (d) control, (e) standard, and (f) high subplot. Diamonds represent the experimental semivariograms for the complete  $\text{NO}_3\text{-N}_{\text{aq}}$  dataset; triangles denote experimental semivariograms computed from the dataset without nondetect samples. Solid lines are the spherical semivariogram models fitted to the experimental variograms of the complete data set.

flow paths of  $\text{NO}_3$  are thought to be predominantly vertical within one layer, the stratigraphic layering may contribute to lateral flows (Iqbal, 2000) leading to both, preferential flow pattern and potentially significant  $\text{NO}_3$  exchange between subplots.

### Spatial Variability of Water Content and Nitrate

#### Water Content

The geometric and zonal anisotropy (Fig. 6) are the result of the highly stratified conditions and strong horizontal layering of water content across the site, which is also evident in the kriged water content map (Fig. 7a, 7b). Such “layering” of moisture content can be the result of either layered strata with significant textural differences and also of transiency in the water flux. The significant contribution of textural layering to the water content distribution suggests that textural differences at the site are the main cause of the water content differences with depth. Similar phenomena have been observed in other field experiments and in numerical studies of vadose flow through heterogeneous media (e.g., Hills et al., 1991; Polmann et al., 1991).

#### Nitrate

Lognormal  $\text{NO}_3\text{-N}_{\text{aq}}$  distributions found at this deep vadose zone site are not unlike those reported in other studies focusing on the root zone (e.g., Tabor et al., 1985; Sharmasarkar et al., 1999; Ilsemann et al., 2001). However, CVs for each subplot treatment (Table 1) are significantly higher than those measured elsewhere, where reported CVs typically range from 20 to 50% and in few cases are as high as 70 to 100% (e.g., Mohanty and Kanwar, 1994; Sharmasarkar et al., 1999; Ilsemann et al., 2001). In part, the higher observed variability of  $\text{NO}_3\text{-N}_{\text{aq}}$  may be attributed to the small sample size (3.5-cm diameter by 7.5-cm length) relative to other typical soil samples ( $\approx 3.2$ -cm diameter by 30-cm length). It may also be a result of the fact that practically all samples are taken at depths well below the mechanical impact

zone of agricultural practices. It cannot be attributed to lithofacies control, since no large concentration contrasts were observed between most lithofacies.

The significantly larger mean  $\text{NO}_3\text{-N}_{\text{aq}}$  of the high subplot indicates that higher than standard fertilizer treatment indeed affects  $\text{NO}_3$  transport to groundwater. However, the difference must be interpreted carefully in light of the high degree of spatial variability. Some of the key patterns in  $\text{NO}_3\text{-N}_{\text{aq}}$  distribution are also due to other boundary effects:

- High concentrations of kriged  $\text{NO}_3\text{-N}_{\text{aq}}$  near the top and in the upper third of the profile of each subplot are attributed to the most recent fertilizer application in 1996 and explain the significant shift in the mean  $\text{NO}_3\text{-N}_{\text{aq}}$  in the upper 3 m (Fig. 5a). In the control subplot, we suspect that the higher  $\text{NO}_3\text{-N}_{\text{aq}}$  content is likely the result of poor root uptake. After 12 yr, tree roots of the control subplot were likely unable to capture the additional N of the one-time application because the root system had grown to capture nutrient supply primarily or exclusively from neighboring treatments (Scott Johnson, personal communication, 2004).
- Significant reduction of the number of nondetects below depths of 12 m is likely the result of the fact that the bottom of the vadose zone had been fully saturated (part of the shallow groundwater system) in some high water years before 1989. Shallow groundwater contains elevated levels of  $\text{NO}_3$  ( $4 \text{ g m}^{-3}$  or more).

Nitrate semivariograms exhibit a statistically significant spatial continuity as postulated in theoretical stochastic models of solute transport through the vadose zone (e.g., Harter and Yeh, 1996). The observed geometric anisotropy may be caused by nonuniform N applications (extrinsic variability). Possibly, such strong geometric anisotropy may also be the result of highly heterogeneous vadose flow processes (see below). While it is difficult to further facilitate the comparison of the results of spatial correlation that we observed for  $\text{NO}_3$

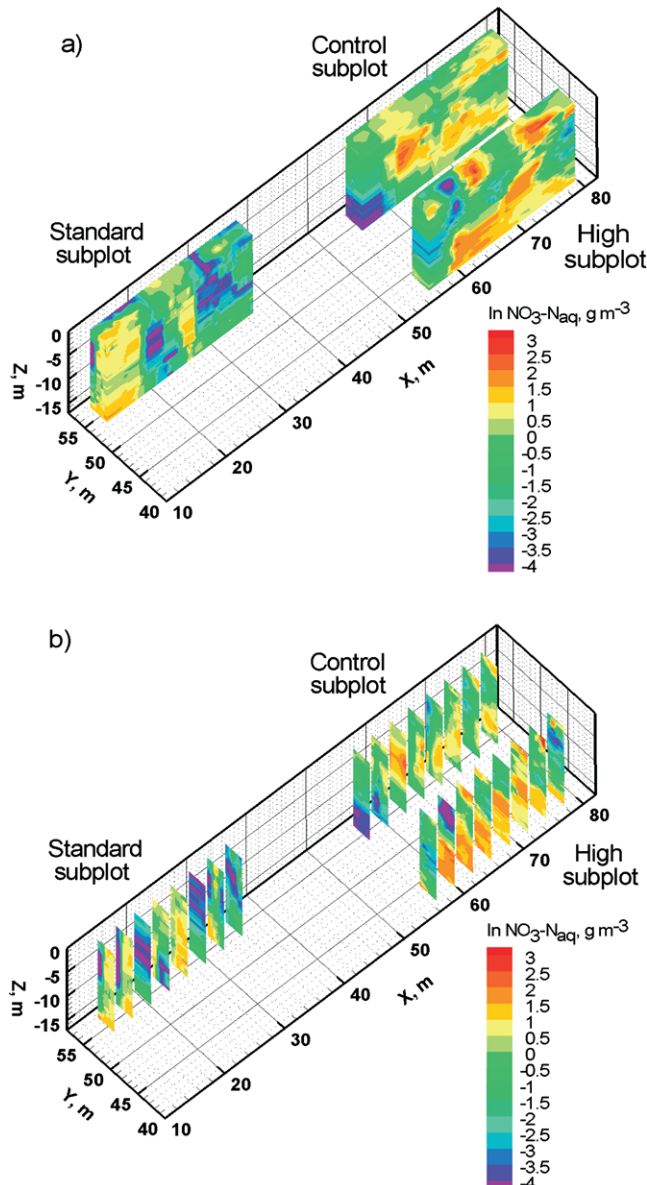


Fig. 9. Contour maps of the kriged (a)  $\ln \text{NO}_3\text{-N}_{\text{aq}}$  ( $\text{g m}^{-3} = \mu\text{g mL}^{-1}$ ) at the control, standard, and high fertilizer treatment sites; (b) various depth profiles of  $\ln \text{NO}_3\text{-N}_{\text{aq}}$  at each subplot.

with those reported by previous studies, it is noteworthy to mention that some studies observed a finite range of spatial dependence (e.g., van Meirvenne and Hofman, 1989). Other studies found monotonically increasing semi-variance with increasing lag distances (e.g., Tabor et al., 1985). In many studies with large sampling distances (10–500 m), a pure nugget effect (no spatial correlation) is observed (e.g., Hofman et al., 1994; Ilsemann et al., 2001; Stenger et al., 2002). This is consistent with our finding that correlation scales of core-measured  $\text{NO}_3\text{-N}_{\text{aq}}$  extend to a few meters at most.

### Spatial Variability of Nitrogen Flux: Interpretation in the Context of Heterogeneous Flow Fields

The probability distributions of  $\theta$  and  $\text{NO}_3\text{-N}_{\text{aq}}$  are consistent not only with root zone field studies but also

with results obtained from stochastic models of flow and transport in heterogeneous porous media. Harter and Yeh (1998) and Harter and Zhang (1999) demonstrated that spatially variable soil properties lead to approximately normal distributed moisture distributions while the resulting vadose moisture velocity distribution is highly skewed (lognormal), which then leads to a skewed concentration distribution. Like its marginal probability distribution, the kriged  $\text{NO}_3\text{-N}_{\text{aq}}$  distribution pattern at the experimental site is also surprisingly similar to that found in other experimental studies (e.g., Hills et al., 1991; Roth et al., 1991) and to that postulated in numerical models (e.g., Harter and Yeh, 1996; Ünlü et al., 1990; Tompson and Gelhar, 1990) of transport in highly heterogeneous hydraulic conductivity fields. We observed zones with individual plumes apparently moving laterally in some locations and downward in others, high concentration variability, and large zones with negligible  $\text{NO}_3$  concentrations.

The conceptual framework of lognormally distributed flow rates (e.g., Harter and Yeh, 1996) is in fundamental contrast to the uniform flow conditions assumed in the LPLN estimates of N mass in the deep vadose zone. Under the conditions of lognormal flow rates (i.e., strongly heterogeneous flux rates), quasipreferential flow paths exist (Polmann et al., 1991; Russo et al., 1994; Harter et al., 1996; Harter and Yeh, 1996), creating a flow pattern not unlike that in soils with a relatively low permeable matrix and a highly permeable macropore structure (Roth et al., 1991). Under such heterogeneous flux conditions, the majority of the pore space is occupied by regions with slow velocities (including stagnant zones that do not contribute significantly to active flow). Nitrate in those low flow regions can have tortuous flow paths, long travel times, and be subject to local denitrification, particularly in the shallow vadose zone after storm events (Pionke and Lowrance, 1991; Ryden and Lund, 1980; Xu et al., 1998; MacQuarrie and Sudicky, 2001). Largest flux contrasts between preferential flow paths and stagnant flow zones would be observed in coarse-textured material because of its low capillary potential. This is consistent with the fact that the largest amount of  $\text{NO}_3\text{-N}_{\text{aq}}$  nondetects at the site occurred in the sand lithofacies S located in the center of the vadose zone profile.

Theoretical models indicate that the relatively high flow zones are of only limited spatial extent (e.g., Fig. 9 in Harter et al., 1996), but their high flux rates lead to rapid  $\text{NO}_3$  transfer through the vadose zone. Such effects of textural heterogeneity on flow nonuniformity are further enhanced by potentially unstable infiltration into the sandy loam root zone, which were documented for this site in Wang et al. (2003). Even stronger instabilities and fingering may occur at and below the interface of fine-textured lithofacies overlying coarse-textured lithofacies (Glass et al., 1988), such as in the deeper sand lithofacies S, which had relatively low water content and a high ratio of  $\text{NO}_3\text{-N}_{\text{aq}}$  nondetects.

The combined evidence of textural heterogeneity, lithofacies contrasts, hydraulic heterogeneity (Minasny et al., 2004), and spatial variability of water content and

$\text{NO}_3\text{-N}_{\text{aq}}$  strongly suggests three major processes controlling the fate and transport of  $\text{NO}_3$  in the vadose zone:

- limited, localized denitrification in the slow flow regions,
- lateral flow and N exchange between subplots, and
- preferential flow and perhaps fingering, which lead to rapid, highly localized N transport toward the water table.

These processes would explain both the large number of nondetects and the overall low N mass remaining in the deep vadose zone. The rapid  $\text{NO}_3\text{-N}_{\text{aq}}$  transport in localized flux channels significantly reduces the amount of N stored in the deep vadose zone, strongly limiting the role of denitrification. Our results suggest that the lack of N stored below the root zone should not automatically be interpreted as significant N attenuation due to denitrification (or other unquantified losses within the root zone). We point out that the conceptual framework of heterogeneous flow (as opposed to uniform deep vadose zone flow) also suggests the simultaneous occurrence of significantly older water next to very young water within the vadose zone. Hence, the  $\text{NO}_3$  distribution at the site (Fig. 9a) represents as much average conditions during the long-term fertilizer treatment (in lower flux regions) as it represents only the most recent two N applications (in 1994, 1996), the latter of which was uniform across all treatments (in the localized high flux regions). This would explain the relative similarity in measured total N levels between subplots.

## CONCLUSIONS

An intensive field sampling campaign resulted in a unique snapshot of the vadose zone  $\text{NO}_3\text{-N}$  distribution throughout its 16-m depth under three different 12-yr fertilization trials. While results are site specific, the site conditions are typical of many agricultural regions in alluvial basins. Our findings summarized below are therefore relevant to heterogeneous, alluvial vadose zone sites below agricultural production areas in general.

1. Significantly higher  $\text{NO}_3\text{-N}$  leaching occurs in overfertilized tree crops, when compared with those fertilized under standard or substandard conditions.
2. The field data reveal significant variability in water content and particularly in the  $\text{NO}_3\text{-N}$  distribution throughout the deep vadose zone, with measured  $\text{NO}_3$  values varying by several orders of magnitude over relatively short distances. Almost one-third of the core samples had nondetectable levels of  $\text{NO}_3\text{-N}$ .
3. Despite the high variability,  $\text{NO}_3\text{-N}$  semivariograms discern the presence of a significant short-range spatial structure at the scale of a several decimeters, particularly in the vertical direction, normal to the horizontal layering in the sedimentary structure. The highly heterogeneous  $\text{NO}_3\text{-N}$  distribution is consistent with the significant textural and hydraulic heterogeneity observed in the vadose zone at the site.
4. The presence of strongly heterogeneous geologic formations at the site, highly variable hydraulic conductivity and water content, and the strongly log-normal, variable distribution of  $\text{NO}_3$  concentrations suggest that highly heterogeneous, skewed or log-normally distributed flux conditions and, in coarse facies, finger-like flow dominate the vadose zone hydrology in these alluvial sediments.
5. The variability of  $\text{NO}_3\text{-N}$  concentrations underscores the importance of high spatial sampling frequencies when monitoring field-scale solute leaching with suction lysimeters or other common soil monitoring tools that measure relatively small volumes of soil water.
6. In alluvial sediments, the often used assumption of uniform flow in the deep vadose zone is inadequate to predict  $\text{NO}_3\text{-N}$  levels in the deep vadose zone below the root zone. Actual  $\text{NO}_3\text{-N}$  levels are potentially much lower due to rapid N transport in preferential flow paths of limited spatial extent.
7. Vice versa, measured  $\text{NO}_3\text{-N}$  levels below the root zone should not be used to validate a LPLN analysis or to close the mass balance of the LPLN framework assuming uniform field-scale flow conditions. Doing so would lead to significant underestimation of  $\text{NO}_3$  leaching rates to groundwater.
8. Denitrification may locally occur throughout the deep vadose zone, but our data indicate that it is not likely to be a major process and cannot account for the relatively low N mass found in the deep vadose zone.
9. Given that field measurements of  $\text{NO}_3\text{-N}$  fluxes below the root zone remain difficult in light of the observed spatial variability, alternative methods for measuring  $\text{NO}_3\text{-N}$  leaching will continue to play a significant role. In particular, proper determination of the field-scale water and N mass balance, independent of root zone  $\text{NO}_3\text{-N}$  measurements, remains an important option. The results also suggest that groundwater quality measurements at the water table are a viable monitoring tool, as travel times through deep vadose zones may be shorter than previously assumed under uniform flow assumptions.

The results are consistent with, albeit not a direct proof of, theoretical work on the effects of soil and sediment heterogeneity on vadose flow and transport. The extensive deep vadose zone sampling campaign presented here provides the first extensive dataset to confirm the applicability of stochastic concepts of unstable flow to predicting solute flux in the deep vadose zone. Ongoing work to substantiate the role of heterogeneity and denitrification will include a detailed, site-specific modeling analysis.

## ACKNOWLEDGMENTS

The research support for this project is provided by the State of California Department of Food and Agriculture Fertilizer Research Education Program, the California Center of Water Resources, and the California Tree Fruit Agreement. We would like to thank Scott Johnson, Katrin Heeren, Anthony Cole, Chad Pyatt, Rigo Rios, Andrea De Lisle, and Timothy

Doane for their help in the collection of the field data and analysis. In particular, we would like to thank Geoprobe Systems for the generous loan of their direct-push drilling rig for this study. We appreciate the helpful comments of several anonymous reviewers and our associate editor, Brian Andraski, which helped to greatly improve this manuscript.

## REFERENCES

- Allaire-Leung, S.E., L. Wu, and B.L. Sanden. 2001. Nitrate leaching and soil nitrate content as affected by irrigation uniformity in a carrot field. *Agric. Water Manage.* 48:37–50.
- Allison, F.E. 1966. The fate of nitrogen added to soils. *Adv. Agron.* 18:219–259.
- Aronsson, P.G. 2001. Dynamics of nitrate leaching and <sup>15</sup>N turnover in intensively fertilized and irrigated basket willow grown in lysimeters. *Biomass Bioenergy* 21:143–154.
- Bar-Yosef, B., and U. Kafkafi. 1972. Rates of growth and nutrient uptake of irrigated corn as affected by N and P fertilization. *Soil Sci. Soc. Am. Proc.* 36:931–936.
- Berthouex, P.M., and L.C. Brown. 1994. *Statistics for environmental engineers.* CRS Press Inc., Boca Raton, FL.
- Blanchard, C.L., and K.A. Tonnesen. 1994. Precipitation chemistry measurements from the California Acid Deposition Monitoring Program, 1985–1990. *Atmos. Environ.* 27A:1755–1763.
- Bransby, D.I., S.B. McLaughlin, and D.J. Parrish. 1998. A review of carbon and nitrogen balances in switchgrass grown for energy. *Biomass Bioenergy* 14:379–384.
- California Department of Water Resources. 2000. California Irrigation Management Information System agricultural resource book. California Dep. Water Resour., Sacramento.
- Cambardella, C.A., T.B. Moorman, J.M. Novak, T.B. Parkin, D.L. Karlen, R.F. Turco, and A.E. Konopka. 1994. Field scale variability of soil properties in central Iowa soils. *Soil Sci. Soc. Am. J.* 58: 1501–1511.
- Dahiya, I.S., R. Anlauf, K.C. Kersebaum, and J. Richter. 1984. Spatial variability of some nutrient constituents of an alfisol from loess. I. Classical statistical analysis. *Z. Pflanzenernaehr. Bodenkd.* 147: 695–703.
- Davis, J.C. 1986. *Statistics and data analysis in geology.* 2nd ed. John Wiley and Sons, New York.
- Deutsch, C.V., and A.G. Journel. 1992. *GSLIB: Geostatistical software library and user's guide.* Oxford University Press, New York.
- de Vos, J.A., D. Hesterberg, and P.A.C. Raats. 2000. Nitrate leaching in a tile-drained silt loam soil. *Soil Sci. Soc. Am. J.* 64:517–527.
- Dowdell, R.J., and C.P. Webster. 1984. A lysimeter study of the fate of fertilizer nitrogen in spring barley crops grown on shallow soil overlying chalk: Denitrification losses and nitrogen balance. *J. Soil Sci.* 35:183–190.
- Frissel, M.J., G.J. Kolenbrander, I. Shvytov, and U.F. Vasileu. 1981. Systematic comparison of the models described. *In* M.J. Frissel and J.A. Van Veen (ed.) *Simulation of nitrogen behavior in soil-plant systems.* Center for Agricultural Publishing and Documentation, Wageningen, the Netherlands.
- Glass, R.J., T.S. Steenhuis, and J.-Y. Parlange. 1988. Wetting front instability as a rapid and far-reaching hydrologic process in the vadose zone. *J. Contam. Hydrol.* 3:207–226.
- Harter, T., A.L. Gutjahr, and T.-C.J. Yeh. 1996. Linearized co-simulation of hydraulic conductivity, pressure head, and flux in saturated and unsaturated, heterogeneous porous media. *J. Hydrol. (Amsterdam)* 183:169–190.
- Harter, T., K. Heeren, G. Weissmann, W.R. Horwath, and J. Hopmans. 1999. Field scale characterization of a heterogeneous, moderately deep vadose zone: The Kearney Research Site. p. 621–630. *In* Proceedings, Characterization and Measurement of the Hydraulic Properties of Vadose Porous Media. U.S. Salinity Lab., Riverside, CA.
- Harter, T., Y.S. Onsoy, K. Heeren, M. Denton, G. Weissmann, J.W. Hopmans, and W.R. Horwath. 2004. Deep vadose zone hydrology in the eastern San Joaquin Valley: At the crossroads between life and mystery. *California Agriculture.*
- Harter, T., and T.-C.J. Yeh. 1996. Stochastic analysis of solute transport in heterogeneous, variably saturated soils. *Water Resour. Res.* 32:1585–1595.
- Harter, T., and T.-C.J. Yeh. 1998. Flow in vadose random porous media nonlinear numerical analysis and comparison to analytical stochastic models. *Adv. Water Resour.* 22:257–272.
- Harter, T., and D. Zhang. 1999. Water flow and solute spreading in heterogeneous soils with spatially variable water content. *Water Resour. Res.* 35:415–426.
- Hauck, R.D. 1981. Nitrogen fertilizer effects on nitrogen cycle processes. p. 551–561. *In* F.E. Clark and T. Rosswall (ed.) *Terrestrial nitrogen cycles.* Ecol. Bull. 33. Swedish Natural Sci. Res. Council., Stockholm, Sweden.
- Hausenbuiller, R.L. 1985. *Soil science principles and practices.* Wm. C. Brown Publ., Dubuque, IA.
- Hills, R.G., P.J. Wierenga, D.B. Hudson, and M.R. Kirkland. 1991. The second Las Cruces trench experiment: Experimental results and two-dimensional flow predictions. *Water Resour. Res.* 27: 2707–2718.
- Hocking, R.R. 1985. *The analysis of linear models.* Brooks/Cole, Monterey, CA.
- Hofman, G., J. De Smet, M. van Meirvenne, and P. Versteegen. 1994. Residual soil nitrate under intensive agriculture. *Commun. Soil Sci. Plant Anal.* 25:1197–1207.
- Horwath, W.R., and E.A. Paul. 1994. Microbial biomass. p. 753–773. *In* Methods of soil analysis. Part 2. SSSA Book Ser. 5. SSSA, Madison, WI.
- Ilseman, J., S. Goeb, and J. Bachmann. 2001. How many soil samples are necessary to obtain a reliable estimate of mean nitrate concentrations in an agricultural field? *J. Plant Nutr. Soil Sci.* 164:585–590.
- Iqbal, M. 2000. Effects of layered heterogeneity in subsurface geologic materials on solute transport under field conditions: A case study from northeastern Iowa, USA. *Hydrogeol. J.* 8:257–270.
- Istok, J.D., J.D. Symth, and A.L. Flint. 1993. Multivariate geostatistical analysis of groundwater contamination: A case history. *Ground Water* 31:63–74.
- Johnson, R.S., F.G. Mitchell, and C.H. Crisost. 1995. Nitrogen fertilization of Fantasia nectarine—A 12 year study. *UC Kearney Tree Fruit Rev.* 1:14–19.
- Krug, E.C., and D. Winstanley. 2002. The need for comprehensive and consistent treatment of the nitrogen cycle in nitrogen cycling and mass balance studies: I. Terrestrial nitrogen cycle. *Sci. Total Environ.* 293:1–29.
- Lafolie, F., L. Bruckler, and A.M. de Corkborne. 1997. Modeling the water transport and nitrogen dynamics in irrigated salad crops. *Irrig. Sci.* 17:95–104.
- Lark, R.M. 2002. Modeling complex soil properties as contaminated regionalized variables. *Geoderma* 106:173–190.
- Legg, J.O., and J.J. Meisinger. 1982. Soil nitrogen budgets. *In* F.J. Stevenson (ed.) *Nitrogen in agricultural soils.* Agron. Monogr. 22. ASA, CSSA, and SSSA, Madison, WI.
- Ling, G., and A.I. El-Kadi. 1998. A lumped parameter model for nitrogen transformation in the vadose zone. *Water Resour. Res.* 34:203–212.
- Lunn, R.J., and R. Mackay. 1994. An integrated modeling system for nitrate transport. *In* Dracos and Stauffer (ed.) *Transport and reactive processes in aquifers.* A.A. Balkema, Rotterdam, the Netherlands.
- MacQuarrie, K.T.B., and E.A. Sudicky. 2001. Multicomponent simulation of wastewater derived nitrogen and carbon in shallow unconfined aquifers. I. Model formulation and performance. *J. Contam. Hydrol.* 47:53–84.
- Martin, D.L., J.R. Gilley, and R.W. Skaggs. 1991. Soil water balance and management. *In* R.F. Follett et al. (ed.) *Managing nitrogen for groundwater quality and farm profitability.* SSSA, Madison, WI.
- Meisinger, J.J., and G.W. Randall. 1991. Estimating nitrogen budgets for soil-crop systems. *In* R.F. Follett et al. (ed.) *Managing nitrogen for groundwater quality and farm profitability.* SSSA, Madison, WI.
- Minasny, B., J.W. Hopmans, T. Harter, S.O. Eching, A. Tuli, and M.A. Denton. 2004. Neural networks prediction of soil hydraulic functions from multi-step outflow data. *Soil Sci. Soc. Am. J.* 68: 417–429.
- Mohanty, B.P., and R.S. Kanwar. 1994. Spatial variability of residual nitrate-nitrogen under two tillage systems in central Iowa: A composite three-dimensional resistant and exploratory approach. *Water Resour. Res.* 30:237–251.
- Mutters, R. 1995. Atmospheric deposition to agricultural soil. *Final*

- Rep. 93-334. California Environmental Protection Agency, Air Resources Board Research Division, Sacramento, CA.
- Olea, R.A. 1999. Geostatistics for engineers and earth scientists. Kluwer Academic Publ., Boston.
- Owens, L.B., W.M. Edwards, and R.W. Vankeuren. 1992. Nitrate levels in shallow groundwater under pastures receiving ammonium nitrate or slow release nitrogen fertilizer. *J. Environ. Qual.* 21: 607-613.
- Page, R.W., and R.A. LeBlanc. 1969. Geology, hydrology, and water quality in the Fresno area, California. USGS Open File Rep. USGS, Reston, VA.
- Paustian, K., O. Andren, M. Clarhom, A.C. Hansson, G. Johansson, J. Lagerlof, T. Lindberg, R. Petterson, and B. Sohlenius. 1990. Carbon and nitrogen budgets for four agro-ecosystems with annual and perennial crops, with and without N fertilization. *J. Appl. Ecol.* 27:60-84.
- Pionke, H.B., and R.R. Lowrance. 1991. Fate of nitrate in subsurface drainage water. *In* R.F. Follett et al. (ed.) Managing nitrogen for groundwater quality and farm profitability. SSSA, Madison, WI.
- Polmann, D.J., D. Mckaughlin, S. Luis, L.W. Gelhar, and R. Ababou. 1991. Stochastic modeling of large-scale flow in heterogeneous unsaturated soils. *Water Resour. Res.* 27:1447-1458.
- Puckett, L.J. 1995. Identifying major sources of nutrient water pollution. *Environ. Sci. Technol.* 29:408A-414A.
- Rao, P.S.C., and R.J. Wagenet. 1985. Spatial variability of pesticides in field soils: Methods for data analysis and consequences. *Weed Sci.* 33:18-24.
- Rees, T.F., D.J. Bright, R.G. Fay, A.H. Christensen, R. Anders, B.S. Baharie, and M.T. Land. 1995. Geohydrology, water quality, and nitrogen geochemistry in the saturated and vadose zones beneath various land uses, Riverside and San Bernadino Counties, California, 1991-93. USGS Water Resources Investigations Rep. 94-4127. USGS, Reston, VA.
- Rolston, D.E., A.N. Sharply, D.W. Toy, and F.E. Broadbent. 1982. Field measurement of denitrification. III. Rates during infiltration cycles. *Soil Sci. Soc. Am. J.* 46:289-296.
- Roth, K., W.A. Jury, H. Fluhler, and W. Attinger. 1991. Transport of chloride through an vadose field soil. *Water Resour. Res.* 27: 2533-2541.
- Russo, D., J. Zaidel, and A. Laufer. 1994. Stochastic analysis of solute transport in partially saturated heterogeneous soil. 1. Numerical experiments. *Water Resour. Res.* 30:769-779.
- Ryden, J.C., and L.J. Lund. 1980. Nature and extent of directly measured denitrification losses from some irrigated vegetable crop production units. *Soil Sci. Soc. Am. J.* 44:501-511.
- Sanchez, L., J.A. Diez, A. Vallho, and M.C. Cartagena. 2001. Denitrification losses from irrigated crops in central Spain. *Soil Biol. Biochem.* 33:1201-1209.
- Sharmasarkar, F.C., S. Sharmasakkar, R. Zhang, G.F. Vance, and S.D. Miller. 1999. Microspatial variability of soil nitrate following nitrogen fertilization and drip irrigation. *Water Air Soil Pollut.* 116:605-619.
- Simek, M., and K.J. Kalcik. 1998. Carbon and nitrate utilization in soils: The effect of long-term fertilization on potential denitrification. *Geoderma* 83:269-280.
- Smith, S.J., and D.K. Cassel. 1991. Estimate nitrate leaching in soil materials. *In* R.F. Follett et al. (ed.) Managing nitrogen for ground-water quality and farm profitability. SSSA, Madison, WI.
- Statsoft, Inc. 2002. STATISTICA 6.0. Statsoft, Tulsa, OK.
- Stenger, R., E. Priesack, and F. Beese. 2002. Spatial variation of nitrate-N and related soil properties at the plot scale. *Geoderma* 105:259-275.
- Stevenson, F.J. 1982. Origin and distribution of nitrogen in soils. p. 1-42. *In* F.J. Stevenson (ed.) Nitrogen in agricultural soils. Agron. Monogr. 22. ASA, CSSA, and SSSA, Madison, WI.
- Stevenson, F.J. 1986. Cycles of soil: Carbon, nitrogen, phosphorus, sulfur, micronutrients. Jon Willey and Sons, New York.
- Tabor, J.A., A.W. Warrick, D.E. Myers, and D.A. Pennigton. 1985. Spatial variability of nitrate in irrigated cotton. II. Soil nitrate and correlated variables. *Soil Sci. Soc. Am. J.* 49:390-394.
- Tanji, K.K., and S.K. Gupta. 1978. Computer simulation modeling for nitrogen in irrigated croplands. p. 79-131. *In* D.R. Nielsen and J.G. MacDonald (ed.) Nitrogen in the environment. Vol. 1. Academic Press, San Diego.
- Tindall, J.A., R.L. Petrusak, and P.B. McMahon. 1995. Nitrate transport and transformation processes in vadose porous media. *J. Hydrol. (Amsterdam)* 169:51-94.
- Trettin, C.C., D.W. Johnson, and D.E. Todd. 1999. Forest nutrient and carbon pools at Walker Branch Watershed: Changes during a 21-year period. *Soil Sci. Soc. Am. J.* 63:1436-1448.
- Tompson, A.F.B., and L.W. Gelhar. 1990. Numerical simulation of solute transport in three-dimensional randomly heterogeneous porous media. *Water Resour. Res.* 26:2541-2562.
- Ünlü, K., D.R. Nielsen, and J.W. Biggar. 1990. Stochastic analysis of vadose flow: One-dimensional Monte Carlo simulations and comparisons with spectral perturbation analysis and field observations. *Water Resour. Res.* 26:2207-2218.
- USEPA. 1990. National water quality inventory. 1988 Report to Congress, EPA-440-4-90-003. USEPA, Washington, DC.
- van Meirvenne, M.V., and G. Hofman. 1989. Spatial variability in topsoil micronutrients in a one ha cropland plot. *Commun. Soil Sci. Plant Anal.* 120:103-110.
- Wang, Z., L. Wu, T. Harter, J. Lu, and W.A. Jury. 2003. A field study of unstable preferential flow during soil water redistribution. *Water Resour. Res.* 39(4):1075. doi:10.1029/2001WR000903.
- Watkins, N., and D. Barraclough. 1996. Gross rates of N mineralization associated with the decomposition of plant residues. *Soil. Biol. Biochem.* 28:169-175.
- Weismann, G.S., S.F. Carle, and G.E. Fogg. 1999. Three dimensional hydrofacies modeling based on soil surveys and transition probability geostatistics. *Water Resour. Res.* 35:1761-1770.
- Wendt, K. 1999. Determination of nitrate/nitrite by flow injection analysis. QuikChem Method 10-107-04-1-A. Lachat Instruments, Milwaukee, WI.
- White, R.E., R.A. Haigh, and J.H. Macduff. 1987. Frequency distribution and spatially dependent variability of ammonium and nitrate concentrations in soil under grazed and ungrazed grassland. *Fert. Res.* 11:193-208.
- Willigen, P., and J.J. Neeteson. 1985. Comparison of six simulation models for the nitrogen cycle in the soil. *Fert. Res.* 8:157-171.
- Xu, C., M.J. Shaffer, and M. Al-Kaisi. 1998. Simulating the impact of management practices on nitrous oxide emissions. *Soil Sci. Soc. Am. J.* 62:736-742.